Article citation info:

Musafir MAA. Ameer ZJA, Hamzah AF. An experimental investigation of fracture modes and delamination behaviour of carbon fiber reinforced laminated composite materials. Diagnostyka. 2023;24(1):2023101. https://doi.org/10.29354/diag/156749.

DIAGNOSTYKA, 2023, Vol. 24, No. 1

e-ISSN 2449-5220
DOI: 10.29354/diag/156749

AN EXPERIMENTAL INVESTIGATION OF FRACTURE MODES AND DELAMINATION BEHAVIOUR OF CARBON FIBER REINFORCED LAMINATED COMPOSITE MATERIALS

Mustafa Abd Alhussein MUSAFIR [1,*], Zuhair Jabbar Abdul AMEER [2], Ahmed Fadhil HAMZAH [3]

[1] Department of Polymers and Petrochemical Industries, Faculty of Materials Engineering, University of Babylon, Iraq
[2] Department of Prosthetics and Orthotics, Faculty of Engineering, University of Karbala, Iraq
[3] Department of Polymers and Petrochemical Industries, Faculty of Materials Engineering, University of Babylon, Iraq
* Corresponding author, e-mail: mat.mustafa.a@uobabylon.edu.iq

Abstract

Mechanically, composite laminates perform exceptionally well in-plane but poorly out-of-plane. Interlaminar damage, known as "delamination," is a major issue for composite laminates. Results from Mode-I and Mode-II experimental testing on twill-woven carbon fiber reinforced (CFRP) laminates are analyzed in this paper. Composite Mode-I fracture toughness was determined using three different methods in accordance with ASTM D5528: modified beam theory, compliance calibration, and a codified compliance calibration. Two methods, the Compliance Calibration Method and the Compliance-Based Beam Method, were used to determine the Mode-II fracture toughness in accordance with ASTM D7905. Stick-slip behavior is quite evident in the composite's Mode-I fracture toughness test findings. The MBT technique's G_{Ic} values for initiation and propagation are 0.533 and 0.679 KJ/m^2, respectively. When comparing the MBT approach to the industry-standard ASTM procedure for determining fracture toughness Mode-I, the MBT method was shown to be highly compatible. Furthermore, the G_{IIc} values for the CBBM technique are 1.65 KJ/m^2 for non-pre cracked and 1.4 KJ/m^2 for pre-cracked materials. The CBBM method shows a good method to evaluate fracture toughness Mode-II, due to not needing to monitor the length of the crack during delamination growth to get the value of the fracture toughness.

Keywords: SCRIMP method, Delamination, Mode-I, Mode-II, Twill woven carbon / epoxy composite.

1. INTRODUCTION

Currently, CFRP composites have superior mechanical qualities including high specific stiffness and high specific strength, they are increasingly employed in a variety of industries. It is well known, for instance, that composite materials account for more than 30% of the Boeing 767's plane structure [1]. When compared to unidirectional CFRP, woven CFRP demonstrates superior impact resistance, shear resistance, and many other benefits.

In spite of the fact that woven CFRP materials have mechanical qualities similar to metals [2], delamination owing to relatively poor resistance to interlaminar failure remains a problem critical. A common failure phenomenon in composites is delamination, which may manifest in a number of different ways depending on factors including the loading speed and type. The considerable loss of compressive strength and structural stiffness brought on by these failure modes has attracted a lot of researchers. When it comes to identifying and analyzing the interlaminar fracture behavior of composite structures in use, delamination is a common issue due to the structure's frequency of occurrence.

The resistance to delamination can be characterized by the transverse tensile strength and the interlaminar shear strength. Delamination resistance can also be measured using a fracture mechanics-based approach, which expresses it as the rate of energy release associated with delamination start and propagation. Tearing, shearing, and opening all promote the propagation of interlaminar delamination.

Thus, the energy release rates in modes I, II, and III, as defined by G_{Ic}, G_{IIc}, and G_{IIIc}, respectively, characterize the delamination fracture toughness of a composite laminate. Studies have mostly concentrated on the more common Mode-I and Mode-II stress levels because Mode III failure is less likely to occur. Testing can be done in a number of ways to figure out things like energy release rate and fracture toughness [3-6].

The interlaminar fracture behavior of composites has been the subject of a large number of experiments over the past few decades.

Rybicki et al. [7] the essential energy release rate was a critical factor in characterizing delamination behavior. Many researchers have further into the concept [8-10]. The majority of these studies used DCB (double cantilever beam) specimens to calculate G_{Ic}. Morais et al. [11,12] and Choi et al.[13] investigated how well DCB testing worked on laminates with multiple orientations. When delamination occurs in multidirectional laminates, it often branches off in several directions or deviates from the center plane, creating a difficult situation. Zulkifli et al.[14] observed interlaminar fracture toughness of the test specimen increased with layer thickness. Aliyu and Daniel [15] examined the mode-I interlaminar toughness of a unidirectional AS4/3501-6 carbon/epoxy using DCB specimens tested to a fracture speed of 51 mm/s. They found that an increase in crack speed meant more toughness. Mustafa et al. [16] analysis of the Mode-I for numbers of stacking sequences (carbon fiber/epoxy). shown the results, the distribution of the G_{Ic} obtained along the delamination front was affected by the ply-angle. As a result, the bending-extension and extension-twisting coupling provide a good of delamination resistance. Ashcroft et al.[17] compared the fracture propagation rates of standard and impact fatigue on a CFRP specimen with mixed-mode crack development and found that the rate of crack propagation was greater during impact fatigue. Funk et al.[18] Analysis of the mode-I fracture toughness of different fabrics demonstrates that the interfacial structure has a major impact on the interlaminar toughness. Kim et al.[19] investigated hybrid composites were shown to have better fracture toughness when compared to both interlock knitted and unweave composites. Pereira et al. [20] study was conducted to establish proper stacking sequences for end-notched flexure (ENF) specimens (Mode-II), shown how G_{IIC} values change with ply angle. Hossein et al. [21] investigated the mode-II interlaminar fracture behavior of various unidirectional carbon/epoxy composites using ENF specimens. Results indicated that the greatest G_{IIc} values, around 1.19 KJ/m^2, were found in high-temperature matrix systems (XHTM45). Results showed that G_{IIc} was increased by 14-27% after post-curing for (MTM).

The experimental testing included the following modes: Mode-I on Double Cantilever Beam (DCB) specimens, and Mode-II on End-Notched Flexure (ENF) specimens. According to ASTM D5528 [6] and ASTM D7905 [22] detail the testing procedures for Mode-I and Mode-II, respectively, are designed for unidirectional composite laminate.

Very little research has been conducted so far to ascertain whether or not these standards may be practically applied to woven CFRP composite. Mode-I fracture toughness assessment for woven composites exhibiting stick-slip behavior has received little attention in experiments. Stick-slip behavior[23] describes fracture propagation in which the crack tip moves forward in a sudden, large step. Because of the lack of knowledge surrounding this behavior, it is essential to investigate the interfacial toughness of composite materials that exhibit it.

Validating the testing result of the fracture toughness Mode-II for woven composite structures is challenging due to the frequent occurrence of unstable delamination growth. This is due to the fact that whether or not the non-adhesive insert functions as a delamination initiator have a significant effect on the attainment of the Mode-II fracture toughness. Mode-II toughness values are rare in the literature because few researchers have planned extended trials to attain them. This is true for both non-pre-crack insert and pre-crack to validate fracture toughness data.

Specifically, this study expands upon the SHRIMP procedure for fabricating the pre-insert twill-woven CFRP laminate. DCB tests and three data reduction procedures; “Modified Beam Theory (MBT)”, “Compliance Calibration (CC)”, and “Modified Compliance Calibration (MCC)” in accordance with standard ASTM D5528 [6]. Furthermore, ENF tests are performed. The delamination development exhibits unclear behavior, necessitating both pre-cracked and non-pre-cracked fracture tests to investigate Mod-II interlaminar fracture toughness's accuracy. Two approaches for data reduction ; “Compliance calibration method (CCM)” and “Compliance-based beam method (CBBM)” in accordance with standard ASTM D7905 [22].

2. MATERIALS AND SPECIMENS

2.1. PRE-cracked panel fabrication

Eighteen layers of twill weave textiles produced from Hexcel's provided carbon fiber AS4 at an area weight of 160 g/m^2 were used to create the CFRP panels with pre-inserts in this study. The panel's thickness was about 3.3 mm, with each layer being around 0.16 mm thick in compliance with the ASTM D5528 and D7905 standard.

To create the insert panel, we used the Seemann Composites Resin Infusion Molding Process (SCRIMP), as showed in figures 1 and 2. To create the pre-insert; (1) an aluminum foil film 12 µm thick was middle in between the 18-ply twill weave carbon fabrics. Before the resin infusion process, the surface of the glass mold was coated with a release agent to improve the demolding process and guarantee the composite panel's surface quality. (2) Release agent, Peel ply, resin flow mesh, and vacuum bagging was stacked to surround the twill weave fabrics with the insert aluminum foil. (3) A vacuum pump machine was used to remove all of the air from the package. (4) The fabric and insert were simultaneously subjected to pressure, which caused the liquid epoxy and hardener to be drawn through the fabric. (5) When all of the textiles had been thoroughly saturated with resin, the flow was stopped and the package was allowed to cure for 24 hours. Carbon fiber volume fraction V_f were 50% depending on the method SCRIMP.

Rectangular specimens were cut from the cured panel and evaluated for elasticity using a universal testing machine according ASTM D3039 [24]. There is a 52.2 GPa modulus in laminate.

2.2. Specimens design

The fracture tests for Mode-I and Mode-II, a 50-mm insert was produced and put into the 180 x 90 mm rectangle panel, as illustrated in figure 3. Figures 4 and 5 illustrate according to ASTM standards-required dimensions for specimens.

3. EXPERIMENTS

3.1. Mode-I test

Fracture toughness Mode-I was measured using double cantilever beam (DCB) specimens and Mode-I loading in accordance with ASTM D 5528-01 to determine the strength of the carbon fiber/interlaminar epoxy composite. Putting together loading blocks with glues epoxy (Araldite 2011A). Test were performed using a universal testing machine equipped with a 5 KN load cell. A very thin layer of opaque white paint was added to both sides of the specimen to enhance visibility of the crack tip. Marks were made 5 mm from the insert's edge, with tiny vertical lines spaced anywhere from once every millimeter to once per eighty millimeters and the length of any crack was calculated from these points. A magnifying glass was used to track the fracture's progress from its tip.

Figure 6 depicts the application of a tensile open load to the specimen (block higher) by raising the grip holding it at a speed rate of (1 mm/min), while holding the lower grip (block lower) steady. In order to observe the growing delamination, the load was remained on the specimen. Determine the delamination length by adding the loading line (the center of the block) distance to the insert's end distance plus the growth increase measured in tick marks.

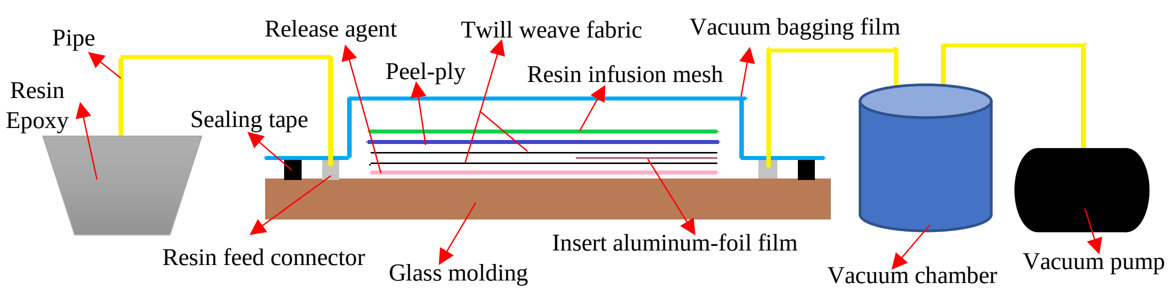

Fig. 1. SCRIMP technique was used to fabricate the pre-inserted CFRP panel

Fig. 2. Steps resin feed for manufacture laminated for DCB and ENF

Two types of Mode-I fracture toughness initiation and propagation were calculated by three methods in the following [6]:

1- MBT method:

$$G_I = \frac{3P\delta}{2b(a+\Delta)} \quad (1)$$

2- CC method:

$$G_I = \frac{nP\delta}{2ba} \quad (2)$$

3- MCC method:

$$G_I = \frac{3P^2C^{2/3}}{2A_1bh} \quad (3)$$

Fig. 3. Laminate the DCB and ENF models

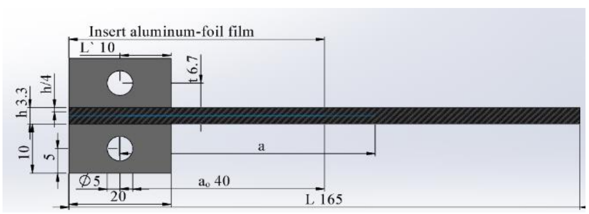

Fig. 4. Scheme in all dimensions according to ASTM for DCB Specimen

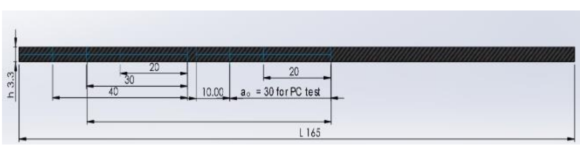

Fig. 5. Scheme in all dimensions according to ASTM for ENF Specimen

Where C is compliance represents the δ́/P ratio; P is load applied; Δ is displacement. b is specimen width; h is specimen thickness; a is the delamination length; A_1 is the slope of the line which generate a least square plot.

3.2. Mode-II test

Fracture toughness Mode-II was measured using three-point end-notched flexural (3ENF) specimens were loaded in Mode-II according to ASTM D7905 to measure the composite carbon fiber /epoxy's interlaminar fracture toughness (G_{IIc}). To perform the test, a universal testing machine with a crosshead speed of 0.5 mm/min and a 5 KN load cell was used. There was a small coat of opaque white paint added to both sides of the specimen to help highlight the crack point. The pre-crack for the subsequent pre-cracked (PC) fracture test, is created during the crack propagation in the specimen during the Non-pre-cracked (NPC) fracture test. Figure 7 depicts the test's main steps.

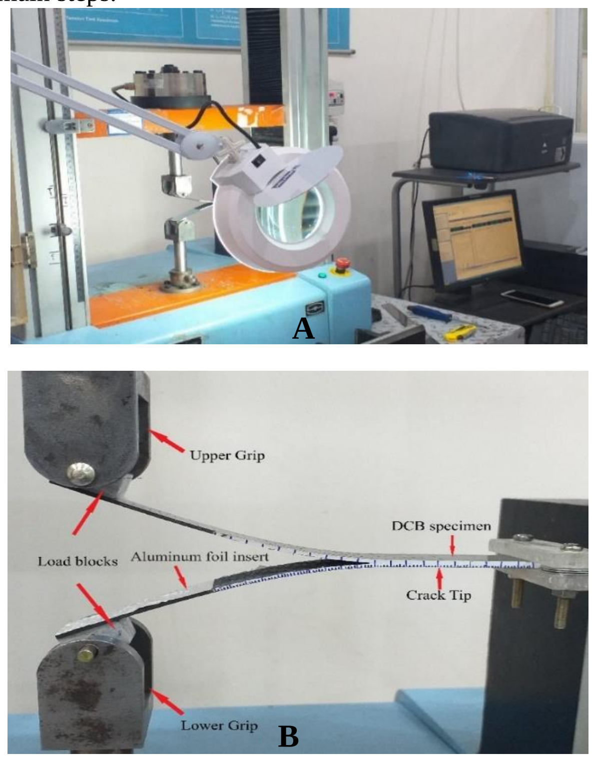

Fig. 6. DCB test: A) Magnifier was utilized to observe the growth delamination, B) During testing DCB specimens

In Figure 7-a; the blue lines are CC markers placed 20 mm and 40 mm in advance of the crack tip, respectively. The loading speed was 0.5 mm/min in displacement control for all CC. CC tests were performed on both NPC and PC before the fracture testing was performed. Half of the predicted critical force at the fracture length of 20 mm was applied to the specimen, and the roller holding the cracked end was aligned with CC marker 1. Afterward, the cracked end's supporting roller was moved so that it faced the CC2 mark. The method followed the same steps as before. As shown in figure 7-a; during both the NPC and PC tests, the supporting rollers were moved to a position 30 mm from the crack tip after the CC tests were completed. Testing of the samples using both NPC and PC is depicted in Figure 8.

The determine of (G_{IIc}) in ENF test, by two methods:

1- CCM method:

$$G_{IIc} = \frac{3mP_{Max}^2a_0^2}{2b} \quad (4)$$

2- CBBM method:

$$G_{\mathrm{IIc}} = \frac{9P^2 a_{eq}^2}{16b^2 E_f h^3} \quad (5)$$

Where m is slop determined using a linear least square linear; P is maximum force from the fracture test; a_0 is delamination length used in the fracture test (30 mm); b is the specimen width; h is specimen thickness; E_{f} is the bending modulus; a_{eq} is equivalent crack length.

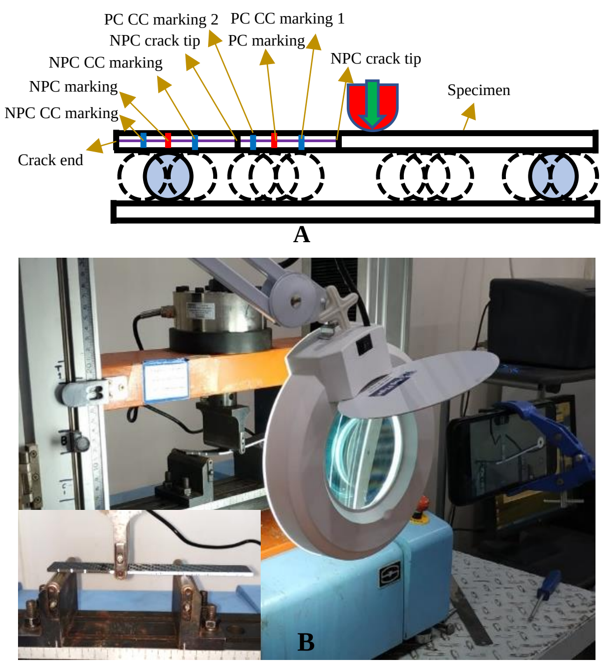

Fig. 7. Mode-II testing (a) Schematic, (b) Photograph of the ENF test setup

4. RESULTS AND DISCUSSION

4.1. Mode-I fracture toughness

The fracture toughness (G_{Ic}) was determined using the Mode-I critical strain energy release rate (SERR). Figure 9 shows the applied load-displacement response of the test specimens; this response was nearly linear in the ascending line up to the inflection point, at which time delamination developed in the DCB specimens' mid-plane. After the linear part, the load's slope flattens out because to crack initiation, but the specimens' load-bearing capacity keeps rising up to a peak load due to fiber bridging. A visible crack propagated upon reaching the peak load, and the applied load dropped off in a zigzag pattern. Due to the difficulty of identifying the exact moment at which a crack began to propagate.

Used three methods to determine crack initiation; first, the point at which the load versus opening displacement curve becomes nonlinear (NL), second, the point at which delamination is observed visually on the specimen edge (VIS), third, the 5% offset. During loading, it was found that the load-displacement curve begins to deviate from linearity in a specific region, therefore this point is considered is NL. It was mainly adopted to represent the crack initiation for generating delamination failure criteria in strength and damage tolerance analyses of laminated composite structures. As for the visual onset of delamination movement on the edge of the specimen represented of VIS, while at the point at which the load has reached a maximum value (5 %/max) represented of 5% offset. NL G_{Ic} values were 14.5 % lower than VIS and 20.27 % than 5 %/max values.

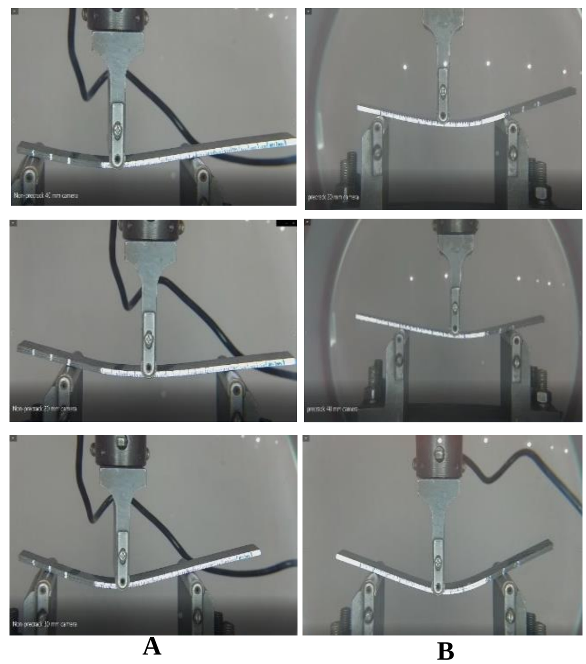

Fig. 8. Mode-II test. A) NPC specimen, B) PC specimen

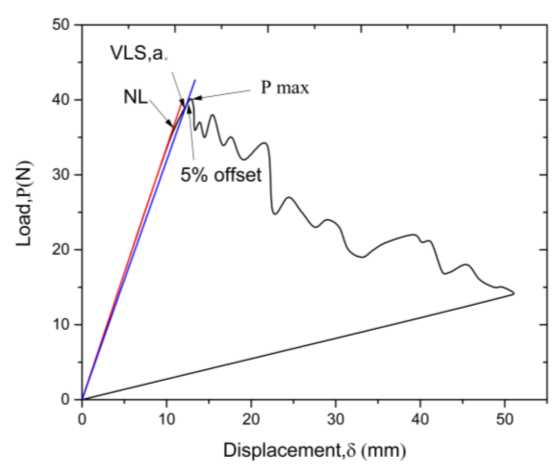

Fig, 9. G_{Ic} (Mode-I) load versus displacement representative curves

The phenomenon of fiber bridging is considered one of the important phenomena during the growth of the delamination in composite materials, because it acts as a shield mechanism to restrict the opening of the fracture surface during the growth of the crack. Therefore, more stress must be used to overcome this restrict, either by pulling the fibers as in DCB or during damage. Figure 10 shows the fibers bridging, it is obvious that there will be a significant amount of bridging fibers present after the delamination front. Fiber bridging are more prominent in the both upper and lower plies of mid plane and in the direction angle 0 of the woven laminates, and therefore have the main role in resisting the growth of the crack because it is located in a direction parallel to the growth of the delamination.

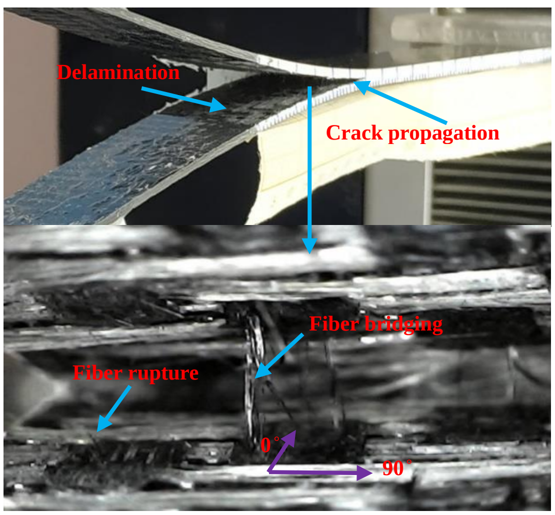

Fig. 10. Digital Microscope: fibers around the delamination zone (fiber bridging) during BCB

As a result, the fracture resistance increases with the development of fiber bridging. Figure 11 which represents a R-curve with the relationship between G_{Ic} and the length of the crack. It can be concluded from the R-curve that the bridging of the fibers can contribute to total strain energy release by increasing the value of G_{Ic} from the initial value corresponding to the crack growth to the plateau after the development of the bridging. Results from the R-curve showed a significant sensitivity to fiber bridging, with G_{Ic} values increasing with fracture length up to a value of 0.704 kJ/m^2.

Three different approaches are used to calculate G_{Ic} during DCB testing, with values of 0.533, 0.547, and 0.604 KJ/m^2 for the MBT, CC, and MCC procedures shown in Figure 12. It's obvious that neither approach is better than the other.

The MBT approach yields results that are on par with those of the CC approach. It was determined that the observed relative fluctuations in G_{Ic} values did not exceed 2.5%. Values of G_{Ic} were found to vary relatively by almost 11.75% and 9.4% when compared to those obtained using the MBT and CC methods, respectively, but only when the MCC method was employed to get these values. Most studies find that the most conservative G_{Ic} values are obtained using the (MBT) method.

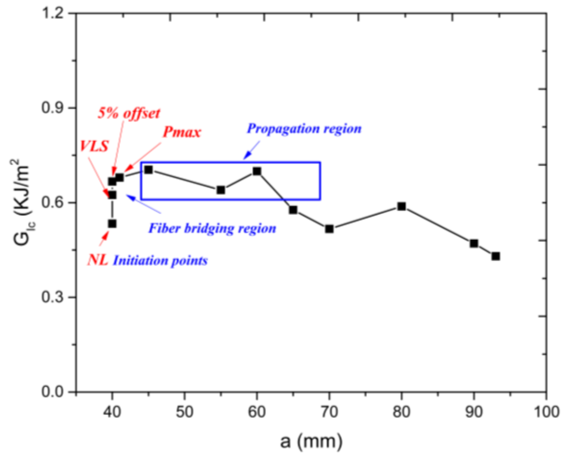

Fig. 11. R-curve, shown effect of fiber bridging on delamination onset and growth by MBT method

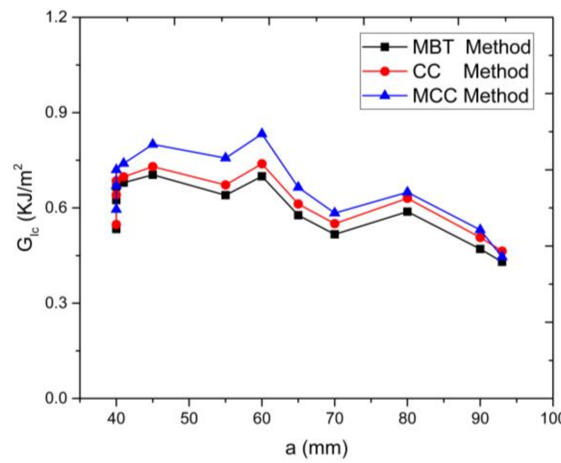

Fig. 12. R-curve, shown G_{Ic} calculation by three methods (MBT, CC and MCC)

As a result, ASTM D5528 recommended the MBT data reduction method as a good alternative to the MCC method for assessing fracture toughness. As a result, the values obtained from the MCC method were neglected in order to get the final G_{Ic} value, and the G_{Ic} value was eventually calculated to be 0.533 KJ/m^2. Figure 13 shown initiation and propagation GIC for each method.

Figure 14 shows the stages of increasing delamination length with increased loading. Table 1 summarizes the results obtained experimentally; they confirm the highest load as the most reliable starting point (NL). Table 2 explained the compared this result study with other authors.

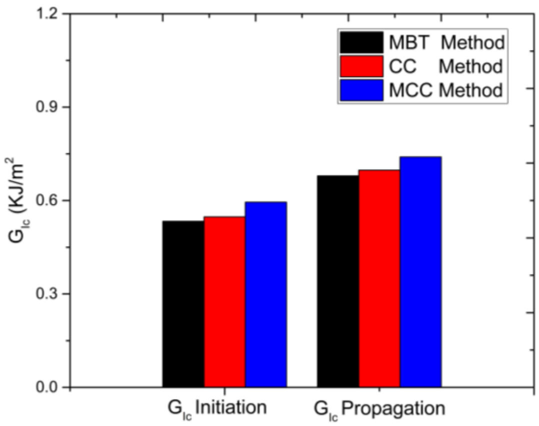

Fig, 13. Shown G_{Ic} initiation and G_{Ic} propagation value for methods (MBT, CC and MCC)

Table 1. Results obtained from the MBT method of Mode-I for CFRP/ Epoxy

	Values
G_{Ic} (KJ/m^2) Initiation (NL)	0.533
G_{Ic} (KJ/m^2) Propagation	0.679
P max (N)	40
Delamination length (mm)	93

4.2 MODE-II FRACTURE TOUGHNESS

The experimental ENF fracture test is separated into two groups: delamination from the pre-implanted insert and delamination from the pre-crack after the delamination has advanced. Use a non-pre cracked (NPC) and pre-cracked (PC) test to find out. The typical load-displacement curve at an NPC test is depicted in Figure 15; the specimen exhibits a linear response with a discernible reduction at the conclusion of the load. When first loaded, a clear but brief non-linear zone appears as a result of the fixture correcting itself. The beginning of the delamination is unstable after the strain energy accumulates over a certain point because of the presence of an "epoxy-rich zone" at the edge of the crack tip. The usual behavior of the sample under the ENF test, in which "in-plane shear" loading causes the surfaces of the mid-plane plies to slide over each other and cause unstable fracture propagation and a quick drop in load [22]. The G_{IIc} at NPC is determined using P_{max} as the critical load point.

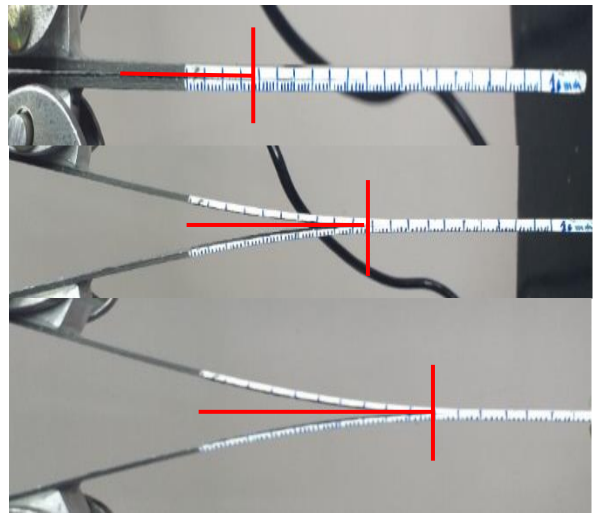

Fig. 14. Delamination length with increasing load

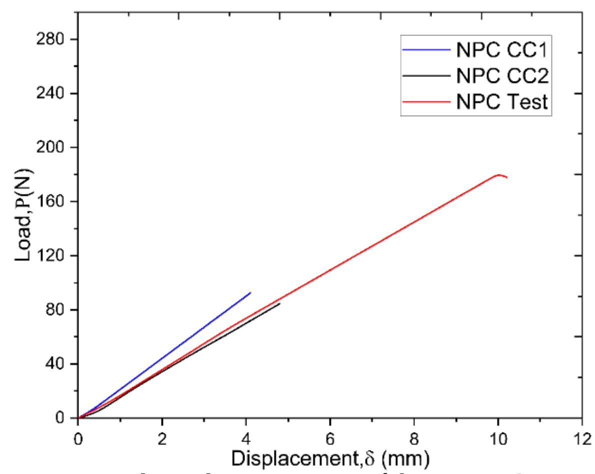

Fig. 15. Load- Displacement curves of the ENF NPC test

Table 2. Values and results from Mode-I testing on CFRP/Epoxy by various authors.

	Current Study	Bensadoun et al. [25]	Saidane et al. [26]	Bensadoun et al. [25]	Liu et al. [27]
Reinforcement	Twill weave	Woven fabrics	Woven fabrics	Woven plies	Plain weave
Matrix	Epoxy	Epoxy	Epoxy	Epoxy	Epoxy
Stiffener	CFRP	CFRP	CFRP	CFRP	CFRP
Composite fabrication	SCRIMP	RTM	CM	RTM	VARI
V_f (%)	50	40	40	40	-
Data reduction method	MBT	MBT	MBT	MBT	MBT
G_{Ic} (KJ/m^2) Initiation	0.533	0.457–0.754	1.07	0.496	0.333-0.634
G_{Ic} (KJ/m^2) Propagation	0.679	1.15–1.59	2.4	0.663	-

"CM: Compression molding", "VARI: Vacuum-assisted resin infusion", "RTM: Resin transfer molding".

Figure 16 is a typical Load-Displacement curve from a PC test; this curve indicates that the specimen loaded linearly at first, indicating that the delamination started in a stable fashion. The load versus displacement curve shows a more pronounced non-linearity before the maximum load point, indicating that the softening stage occurs before the maximum load point. After the pre-crack, the crack can happen more predictably. Thus, the behavior of crack formation in the (PC) test is different from that in the (NPC) test, as will be briefly apparated.

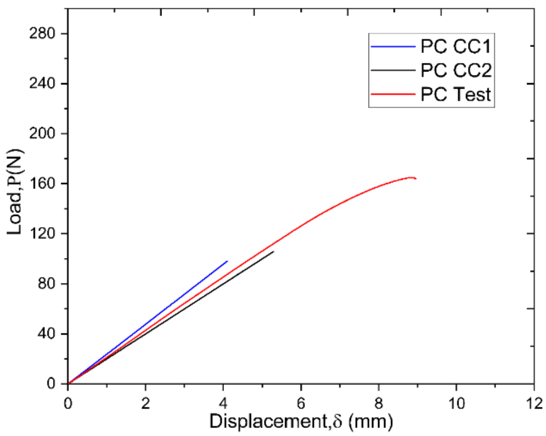

Fig. 16. Load- Displacement curves of the ENF PC test

For the purpose of determining the G_{IIc} at PC, Pmax is assumed to be the critical load point. Figure 17 depicts the development of cracks and the resulting sliding of layers.

After an NPC fracture test, a new loading position for the PC test must be determined by marking the location of the crack tip. Therefore, a compliance calibration (CC) test must be performed when employing the compliance calibration method (CCM) to determine CC coefficients (CC1 at 20 mm, CC2 at 40 mm, $a_0$at 30 mm) for NPC test. also, for PC test determine CC coefficients (CC1 at 20 mm, CC2 at 40 mm, a_{calc} at 30 mm). The G_{IIc} was calculated using two method and the averaged results of valid NPC and PC test are presented in Table 3. The averaged results (NPC and PC) are in the same range and overlap, as can be seen when taking the variations into account.

Table 3. Comparison of the G_{IIc} obtained from the CBBM and CCM at NPC and PC.

Mean	G_{IIc} NPC (KJ/m^2)	G_{IIc} PC (KJ/m^2)	G_{IIc}(Average) (KJ/m^2)
CCM	1.34	1.07	1.205
CBBM	1.65	1.4	1.52
Deviation %	18	25	

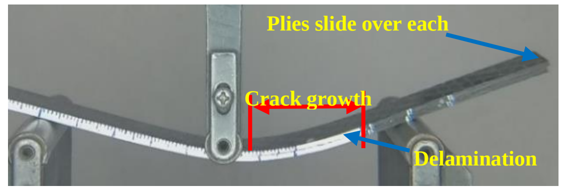

Fig. 17. Delamination growth during ENF test

5. CONCLUSIONS

In this study, according to ASTM D5528 calculate the Mode-I initial and propagation fracture toughness G_{Ic} value for a twill-woven CFRP that exhibits stick-slip behavior during the growth of delamination. When comparing the three approaches used to minimize the data on Mode-I fracture toughness, it was observed that the MCC method yielded the highest fracture toughness value. When comparing them using the CC approach, however, the difference in fracture toughness was clearly visible. Given that the MBT approach is a reliable alternative for gauging fracture toughness in Mode-I, it seems sense that it was the most cautious of the available options.

Furthermore, Mode-II fracture toughness tests were conducted successfully using NPC and PC according to ASTM D7905, with results that converged, demonstrating the validity of the Mode-II fracture toughness data. Two methods were used to reduce the data on fracture toughness Mode-II, the CBBM method showed more variation than the CCM method. Therefore, it is preferable to use a CBBM method because it does not need to monitor the length of the crack during delamination to determine the value of the fracture toughness for Mode-II. In conclusion, the ASTM D5528 for Mod-I and ASTM D7905 for Mod-II are proven to be effective standards to determine fracture toughness for twill-woven CFRP.

Table 4. Values and results from Mode-II testing on CFRP/Epoxy by various authors

	Current study	Bensadoun et al. [25]	Rajendran et al. [28]	Liu et al. [29]
Reinforcement	Twill weave	Weave fabrics	Plain weave fabrics	Weave fabrics
Matrix	Epoxy	Epoxy	Epoxy	Epoxy
Stiffener	CFRP	CFRP	CFRP	CFRP
Composite fabrication	SCRIMP	RTM	Hand- layup	Prepreg
V_f (%)	50	40	0.44	64.2
Data reduction method	CCM/CBBM	CBT	CCM	CCM/CBT/CBM
G_{Ic} (KJ/m^2)	1.205/1.52	1.315-1.872	0.962	1.37/ 1.4/ 1.42

However, CBBM method shown the PC and NPC findings have a greater variation from CCM method. Therefore, it can be stated that in the experimental test, the CCM approach requires monitoring of the crack propagation length while the CBBM method does not. [30]. Several studies have shown that CBBM's measurements of G_{IIc} are more accurate than those made using other methods [31]. Table 4 explained the compared this result study with other authors.

Author contributions: *research concept and design, M.A.A.M.; Collection and/or assembly of data, M.A.A.M.; Data analysis and interpretation, M.A.A.M.; Writing the article, M.A.A.M.; Critical revision of the article, Z.J.A.A.; A.F.H.; Final approval of the article, Z.J.A.A.; A.F.H.*

Declaration of competing interest: *The authors declare that they have no known competing financial interests or personal relationships that could have appeared to influence the work reported in this paper.*

REFERENCES

1. Hocheng H, Tsao CC. The path towards delamination-free drilling of composite materials. J. Mater. Process. Technol. 2005;167(2–3):251–264. https://doi.org/10.1016/j.jmatprotec.2005.06.039.
2. Jacob GC, Starbuck JM, Fellers FJ, Simunovic S, Boeman RG, The effect of loading rate on the fracture toughness of fiber reinforced polymer composites. J. Appl. Polym. Sci. 2005;96(3):899–904. https://doi.org/10.1002/app.21535.
3. Asp LE. The effects of moisture and temperature on the interlaminar delamination toughness of a carbon/epoxy composite. Compos. Sci. Technol. 1998;58(6):967–977. https://doi.org/10.1016/S0266-3538(97)00222-4.
4. Shivakumar KN, Crews JH, Avvat VS. Modified mixed-mode bending test apparatus for measuring delamination fracture toughness of laminated composites. J. Compos. Mater. 1998;32(9):804–828. https://doi.org/10.1177/002199839803200901.
5. Crews JH, Reeder JR. A mixed-mode bending apparatus for delamination testing. NASA Ames Res. Cent. 1981;1000: 19890001574.
6. A. International. ASTM D5528-01 (Standard test method for mode I interlaminar fracture toughness of unidirectional fiber-reinforced polymer matrix). 2014.
7. Rybicki EF, Schmueser DW, Fox J. An energy release rate approach for stable crack growth in the free-edge delamination problem. J. Compos. Mater. 1977;11(4): 470–487. https://doi.org/10.1177/002199837701100409.
8. Davitt DF, Schapery RA, Bradley WL. A method for determining mode 1 delamination fracture toughness of elastic and viscoelastic composite materials. J. Comp. Mat. 1980;14:270–285.
9. Davies P, Moulin C, Kausch HH, Fischer M, Measurement of GIc and GIIc in carbon/epoxy composites. Compos. Sci. Technol. 1990;39(3): 193–205. https://doi.org/10.1016/0266-3538(90)90041-3.
10. Caprino G, The use of thin DCB specimens for measuring mode I interlaminar fracture toughness of composite materials. Compos. Sci. Technol. 1990;39(2):147–158 https://doi.org/10.1016/0266-3538(90)90052-7.
11. De Morais AB. Double cantilever beam testing of multidirectional laminates. Compos. Part A Appl. Sci. Manuf. 2003;34(1):1135–1142. https://doi.org/10.1016/j.compositesa.2003.08.008.
12. Pereira AB, de Morais AB. Mode I interlaminar fracture of carbon/epoxy multidirectional laminates. Composites Science and Technology. 2004;64(13-14):2261–2270 https://doi.org/10.1016/j.compscitech.2004.03.001.
13. Choi JKG, Williams NS. Delamination fracture of multidirectional carbon-fiber epoxy composites under mode I, mode II and mixed-mode I-II loading. J. Compos. Mater. 199;33(1):73–99.
14. Zulkifli R, Azhari CH, Ghazali MJ, Ismail AR, Sulong AB. Interlaminar fracture toughness of multi-layer woven silk/epoxy composites treated with coupling agent. Eur. J. Sci. Res. 2009;27:454–462.
15. Aliyu AA, Daniel IM. Effects of strain rate on delamination fracture toughness of graphite/epoxy. Delamination Debonding Mater. Johnson. 1985: 336–348.
16. Alhussein MA, Ameer ZA, Hamzah AF. Simulation of the effect laminate sequence on delamination mode-I with elastic couplings. Diagnostyka. 2922;23(2):1–12. https://doi.org/10.29354/diag/150547.
17. Ashcroft IA, Casas-Rodriguez JP, Silberschmidt VV. Mixed-mode crack growth in bonded composite joints under standard and impact-fatigue loading. J. Mater. Sci. 2008;43(2):6704–6713. https://doi.org/10.1007/s10853-008-2646-6.
18. Funk JG The interlaminar fracture toughness of woven graphite/epoxy composites. 1989.
19. Kim KY, Ye L. Interlaminar fracture properties of weft-knitted/woven fabric interply hybrid composite materials. J. Mater. Sci. 2012;47(20): 7280–7290. https://doi.org/10.1007/s10853-012-6682-x.
20. Pereira AB, De Morais AB. Mode II interlaminar fracture of glass/epoxy multidirectional laminates. Composites Part A: Applied Science and Manufacturing. 2004;35(2):265–272. https://doi.org/10.1016/j.compositesa.2003.09.028.
21. Saidpour H, Barikani M, Sezen M. Mode-II Interlaminar Fracture Toughness of," Iran. Polym. J. 2003;2(5):389–400. http://roar.uel.ac.uk/1033/1/Saidpour%2CH%282003%29IPJ12%285%29389.pdf
22. A International. ASTM D7905/D7905M-14 (Standard Test Method for Determination of the Mode II Interlaminar Fracture Toughness of Unidirectional Fiber-Reinforced Polymer). 2014.
23. Dalbe MJ, Santucci S, Cortet PP, Vanel L. Strong dynamical effects during stick-slip adhesive peeling. Soft Matter. 2014;10(1):132–138. https://doi.org/10.1039/c3sm51918j.
24. A. International. ASTM D3039 (Standard Test Method for Tensile Properties of Polymer Matrix Composite Materials). 2014.

25. Bensadoun F, Verpoest I, Van Vuure A. Interlaminar fracture toughness of flax-epoxy composites. Journal of Reinforced Plastics and Composites. 2017;36(2):121-136. https://doi.org/10.1177/0731684416672925.
26. Saidane R, Scida EH, Pac D, Ayad MJ. Mode-I interlaminar fracture toughness of flax, glass and hybrid flax-glass fibre woven composites: failure mechanism evaluation using. acoustic emission analysis. Polymer Testing. 2019;75:246–2539. https://doi.org/10.1016/j.polymertesting.2019.02.022.
27. Liu Z, Xia Y, Guo S. Characterization methods of delamination in a plain woven CFRP composite. J. Mater. Sci. 2019;54(20):13157–13174. https://doi.org/10.1007/s10853-019-03847-4.
28. Rajendran TS, Johar M, Low KO, Hassan SA, Wong KJ. Interlaminar fracture toughness of a plain weave flax/epoxy composite. Plast. Rubber Compos. 2019;48(2):74–81. https://doi.org/10.1080/14658011.2018.1550235.
29. Liu C, Bai R, Lei Z, Di J, Wu W, Zou J, Gao T, Yan C. Mode II fracture toughness related to ply angle for composite delamination analysis. Mechanics of Advanced Materials and Structures. 2021;28(23):2417–2428. https://doi.org/10.1080/15376494.2020.1740955.
30. Ducept F, Davies P, Gamby D. Mixed mode failure criteria for a glass/epoxy composite and an adhesively bonded composite/composite joint. International Journal of Adhesion and Adhesives. 2000;20(3):233–244. https://doi.org/10.1016/S0143-7496(99)00048-2.
31. de Moura MFSF, Campilho RDSG, Gonçalves JPM. Crack equivalent concept applied to the fracture characterization of bonded joints under pure mode I loading. Composites Science and Technology. 2008; 68(10–11):2224–2230,2008. https://doi.org/10.1016/j.compscitech.2008.04.003.

Received 2022-09-23
Accepted 2022-11-24
Available online 2022-11-01

Mustafa Abdul Hussein MUSAFIR was born in Hilla, Iraq in 1990-lecturer at the University of Babylon in the materials engineering field, He got his B.Sc. degree in materials engineering in 2014, and received his M.Sc. in materials engineering also in 2018 from the University of Babylon, and Now a Ph.D student in the research in materials engineering (composite materials) in at University of Babylon.

Zuhair Jabbar Abdul AMEER is currently a professor of Prosthetics and Orthotics Engineering Department at University of Kerbala, College of Engineering. I earned my B.Sc. in engineering and metals production in 1992 from University of Technology, M.Sc. and Ph.D. in materials engineering in 2001 and 2007 from Babylon University.

Ahmed Fadhil HAMZAH – Professor at the University of Babylon in the materials engineering field, He got his B.Sc. degree in materials engineering in 2004, and received his M.Sc. in materials engineering also in 2007 from the University of Babylon, and his Ph.D. in materials engineering (composite materials) in 2013 at University of Technology.